IIETA International Information and Engineering Technology Association
Advancing the World of Information and Engineering

Instrumentation Mesure Métrologie
Vol. 25, No. 1, February, 2026, pp. 9-18
Journal homepage: http://iieta.org/journals/i2m

A Metrologically-Grounded Analysis of Bridge-Type Bucket-Wheel Excavator Degradation under Variable Operating Conditions

Ammar Gouri[1*], Abdallah Kabouche[1], Azzeddine Dekhane[2], Chouaib Rahli[1], Ahmed Bouraiou[3], Yahia Bousseloub[1]

[1] LSEM, Laboratory of Electromechanical Systems, Badji Mokhtar – Annaba University, Annaba 23000, Algeria
[2] National Higher School of Technology and Engineering, Annaba 23005, Algeria
[3] Renewable Energy Research Unit in Saharan Environment (URERMS), Renewable Energy Development Center (CDER), Adrar 01000, Algeria

Corresponding Author Email: amar.gouri@univ-annaba.dz

https://doi.org/10.18280/i2m.250102

Received: 26 November 2025
Revised: 14 January 2026
Accepted: 23 January 2026
Available online: 28 February 2026

Keywords:
measurement uncertainty, wear metrology, dimensional measurement, in-situ monitoring, calibration traceability, bucket-wheel excavator, degradation analysis, reliability assessment

ABSTRACT

This paper presents a metrologically grounded analysis of degradation in bridge-type bucket-wheel excavators (BWEs) operating under variable industrial conditions. These systems, widely used in iron-ore handling, are exposed to severe mechanical loads, abrasive contacts, and moisture-related operating conditions that accelerate component degradation and reduce reliability. The study combines calibrated wear measurements with stated uncertainty, grouped industrial failure data, and discrete-event simulation to investigate the relationship between operating conditions and degradation behavior. Wear measurements were performed on four support rollers using a calibrated digital vernier caliper with traceable uncertainty evaluation. Historical maintenance records were analyzed to identify the most degradation-prone components and to determine the correlation between operating load and failure occurrence. Statistical analysis showed that higher production loads are associated with increased failure frequency, particularly in the bucket-wheel subsystem. In parallel, experimental observations indicated that higher ore moisture content accelerates wear progression. A simulation framework was also developed to evaluate the effects of different production-flow scenarios on system reliability, downtime, and mission completion time. The results demonstrate that heavy operating loads and wetter service conditions are associated with faster wear evolution and more unfavorable reliability outcomes. The proposed framework provides a measurement-based basis for reliability-informed maintenance assessment in mining equipment systems.

1. INTRODUCTION

Bridge-type bucket-wheel excavators (BWEs) are essential machinery in large-scale mining and material handling, where they operate under heavy mechanical stresses and environmental challenges. These machines, used primarily in the extraction of iron ore, face varying loads and operating conditions that lead to progressive wear and frequent failures. The critical components of BWEs, including the bucket wheel, rollers, and carriages, are subjected to abrasive contact, fluctuating loads, and humidity variations, which accelerate degradation and reduce operational reliability over time.

Previous research on BWEs has primarily focused on structural integrity assessments, failure analysis, and maintenance optimization for individual components. Studies such as the previous studies [1-4] have investigated the failure mechanisms of bucket wheel components, including fatigue and wear, while others have addressed specific damage modes such as fracture in pulley systems [5] and crack propagation in the boom [6]. These efforts have provided valuable insights into the damage mechanisms and operational challenges faced by BWEs, but most have been limited by deterministic assumptions, focusing on individual components or static load profiles. As a result, they often fail to capture the dynamic and interactive nature of degradation mechanisms that occur in real-world operational environments. For example, recent reliability analyses of mining machinery highlight that complex systems operating under varying loads exhibit highly stochastic failure behavior, underscoring the need for probabilistic degradation modeling rather than static assumptions [7].

Wear is a major degradation mechanism in BWEs and is influenced by operating load, contact conditions, and moisture-related service conditions [8-10]. Although previous studies have reported valuable results on structural failure, component damage, and maintenance issues in BWEs, these studies have generally treated wear analysis, reliability assessment, and operational modeling separately. As a result, the link between metrologically controlled wear observations and system-level degradation analysis under variable operating conditions remains insufficiently developed [11, 12]. The contribution of the present study is therefore not the

proposal of a universal degradation law for all BWEs, but the development of a case-specific analytical framework in which calibrated wear measurements with stated uncertainty are combined with field failure data and discrete-event simulation to examine how operating conditions are associated with degradation behavior and reliability in one bridge-type BWE system. In this framework, load and moisture-related conditions are considered jointly at the level of scenario analysis and degradation interpretation, rather than through a fully estimated multivariate stochastic intensity model. The objective is to provide a measurement-grounded basis for reliability-informed interpretation of degradation trends under realistic industrial conditions [13, 14].

The remainder of the paper is organized as follows. Section 2 describes the investigated system and its operating context. Section 3 presents the degradation-modeling assumptions. Section 4 details the measurement methodology and metrological framework. Section 5 reports the statistical analysis of failure data. Section 6 presents the experimental wear study, and Section 7 reports the simulation-based production and reliability analysis. Section 8 discusses the results, limitations, and implications, and Section 9 concludes the paper.

A distinguishing feature of the present study is the integration of calibrated wear measurements with stated uncertainty into the degradation and reliability analysis of the investigated BWE system.

2. SYSTEM DESCRIPTION AND OPERATIONAL CONTEXT

The bridge-type BWE system under study is utilized for iron ore handling in large-scale mining operations. The system operates under harsh environmental conditions, including fluctuating operating loads and environmental humidity, which significantly influence the degradation of key components. The system consists of three primary subsystems: the bucket wheel, the carriage, and the bridge.

Component Degradation: Historical maintenance records indicate that failures were concentrated in the bucket-wheel subsystem, with support rollers identified as the most degradation-prone components in the investigated system. This is consistent with the fact that support rollers are directly exposed to severe mechanical stresses and moisture-related operating conditions that may aggravate wear.

Operating Conditions: Seasonal variations in failure rates suggest sensitivity to moisture-related service conditions. In the present study, the quantity previously referred to as humidity corresponds to the moisture content of the handled iron ore, not ambient relative humidity. The maximum recorded ore moisture content during the observation period was 7.6%. This operating variable is considered in the degradation analysis together with load and operating duration.

Technical Characteristics: The operational parameters of the BWE system, summarized in Table 1, define the operational envelope within which degradation and reliability analyses are conducted. These parameters include throughput capacity, wheel rotation speed, and material properties, among others. The environmental conditions, such as humidity and temperature ranges, are also crucial for linking the system's performance to degradation modeling and reliability analysis.

Figure 1 illustrates the overall configuration of the BWE, highlighting the key components, particularly the support rollers, which are the most degradation-prone parts. The figure visually emphasizes how environmental factors, such as humidity, directly impact these components, accelerating wear and reducing overall system reliability.

Table 1. Technical specifications bucket-wheel reclaimer system model BR-650-35-N-1-W-5

Parameter	Specification
Throughput	1100 tons/h
Wheel Rotation Speed	4.3 rev/min
Number of Buckets	10 buckets
Bucket Discharge Rate	43 buckets/min
Wheel Diameter	4750 mm
Linear Wheel Speed	1.06 m/s
Bridge Advance Speed	0.10 – 0.45 m/s
Carriage Travel Speed	1 – 10 m/min
Material Handled	Iron ore
Granulometry	0 – 10 mm
Bulk Density	1.7 t/m³
Maximum ore moisture content	7.6%

Figure 1. Wheel excavator with bridge-type bucket for the iron ore reclaiming process

3. DEGRADATION MODELING ASSUMPTIONS

3.1 Wear model

To represent the progressive loss of material in the roller elements, the present study adopts the Archard wear framework. In this formulation, material removal depends on the contact load, the relative sliding path, and the resistance of the softer surface to deformation [10]. For the operating intervals considered here, the wear depth is treated as approximately linear with time. This simplification is appropriate for the normal service regime investigated in the experimental campaign and provides a practical basis for linking measured wear to system-level degradation behavior [12, 15-19].

3.2 Assumption on the impact of load and sliding velocity on wear

The abrasive wear formulation follows classical Archard-based tribological models [10, 15, 17].

It is assumed that the operating load applied to the production system significantly influences the wear rate. As the load increases, the extent of component wear also increases, which in turn raises the likelihood of failure. Under mechanical friction conditions involving two-body abrasive wear, the worn volume V (m^3) is directly related to the normal load F_N (N) and the sliding distance L (m), and inversely related to the hardness H ($N \cdot m^{-2}$) of the softer contacting surface. Accordingly, the abrasive wear volume can be

expressed as follows [15, 16].

$$V = \frac{K_a F_N L}{H_s} = \frac{G}{\gamma} \quad (1)$$

where, G (kg) represents the weight loss, γ (kg/m³) denotes the material density, and V/L (m³/m) corresponds to the volumetric wear rate. In tribological systems characterized by frictional contact between a hard surface and a significantly softer counter-surface, wear mainly affects the softer material. Nevertheless, the resulting worn volume cannot be predicted reliably by deterministic formulations alone.

The wear coefficient formulation is commonly adopted in tribology studies [12, 15].

In real-world conditions, the wear factor K (m²/N) is a practical approach to describing wear and is more widely used than the K_a/H_s ratio, which has less applicability across varying operational scenarios. The relationship is therefore expressed as:

$$K = \frac{K_a F_N L}{H_s} = \frac{V}{F_N L} \quad (2)$$

This assumption is commonly used for plastic contact conditions in tribological systems [11, 15].

Under conditions of plastic deformation, the normal contact pressure may be assumed to be approximately equal to the hardness H_s of the worn material. On this basis, the total real contact area can be written as follows:

$$A_s = \frac{F_N}{H_s} \quad (3)$$

By combining Eqs. (1) and (3), the abrasive wear volume of the material can be expressed as follows:

$$V = K_a A_r L \quad (4)$$

The sliding distance may be expressed as $L = v \times t$, where v (m/s) is the sliding velocity and t (s) is the duration of the wear process. Similarly, the normal load F_N on the contact interface is given by $F_N = p \times A$, where p (N·m^{-2}) denotes the average contact pressure and A (m^2) refers to the nominal contact area.

Substituting these expressions into Eq. (1) yields:

$$V = \frac{K_a F_N L}{H_s} = \frac{K_a (vt) F_N}{H_s} = \frac{K_a (vt) pA}{H_s} = \frac{K_a (pA) tv}{H_s} \quad (5)$$

The thickness h (m) of the linear wear quantity can be expressed as follows:

$$h = \frac{V}{A} = \frac{K_a (pv) t}{H_s} = \frac{G}{A\gamma} \quad (6)$$

The linear wear rate, or wear intensity, is defined by the ratio h/L (mm^{-1}). When the wear depth h is used as the reference quantity for characterizing wear evolution, the time-dependent wear rate may be written as $\lambda = dh/dt$ [16, 18]. For most engineering calculations, a linear relation between wear depth h and operating time t can be assumed. This means that, during the normal service period, the wear rate remains approximately constant. Under this assumption, the wear evolution with time may be simplified as $\lambda = h/t$. Therefore, the wear rate as a function of time can be expressed as follows:

$$\lambda = \frac{h}{t} = \frac{K_a (pv)}{H_s} \quad (7)$$

In this study, h denotes the linear wear depth and λ denotes the corresponding wear rate expressed as wear-depth change over time. Under the assumption of approximately steady operating conditions over short intervals, λ is interpreted as a local average wear rate used to compare degradation behavior under different operating conditions.

3.3 Stochastic representation of degradation

The Archard-based formulation presented above is used in this study as a mechanistic basis for interpreting wear progression under different operating conditions. However, the present manuscript does not estimate a fully parameterized stochastic degradation process directly from the wear data. Instead, degradation variability is represented more cautiously through the combined interpretation of measured wear, grouped failure records, and simulation-based operating scenarios.

Within this framework, load and moisture-related conditions are introduced as operating variables associated with changes in wear behavior and failure occurrence. Their role is therefore interpretive and comparative rather than that of formally estimated covariates in a validated stochastic intensity function. Accordingly, the model should be understood as a measurement-grounded degradation-assessment framework rather than as a fully specified stochastic process model with identified distributional form and parameter-estimation procedure.

This clarification is important for the interpretation of the results. The manuscript supports the conclusion that varying operating conditions are associated with different degradation trends in the investigated BWE system, but it does not claim to establish a universally parameterized stochastic wear law for broader direct transfer without further model identification and validation.

4. MEASUREMENT METHODOLOGY AND METROLOGICAL FRAMEWORK

The measurement methodology combines precise instrumentation, experimental data collection, and analytical tools to ensure reliable wear assessment. Figure 2 illustrates the measurement device, the tested components, and the industrial environment of the BWE. It also presents sample data and graphical analysis used to evaluate wear evolution and variability. This integrated approach links real measurements with data analysis and modeling, ensuring accuracy, traceability, and consistency in the degradation assessment.

4.1 Instrumentation and calibration protocol

All dimensional measurements were performed using a digital vernier caliper (Mitutoyo series 500-196-30) with a resolution of 0.01 mm and an accuracy of ±0.02 mm, calibrated traceably to national standards. The calibration certificate (No. CAL-2023-045) confirms compliance with ISO 13385-1:2011 requirements, with calibration intervals of

3 months to ensure measurement integrity throughout the 11-month study period.

Table 2. Metrological characteristics of the wear depth measurement system

Wear Depth	Specification
Instrument/System	Digital Vernier Caliper
Range	0 – 150 mm
Resolution	0.01 mm
Accuracy/Uncertainty	±0.11 mm (U95, k = 2)
Calibration standard	ISO 13385-1:2011
Calibration interval	3 months

The metrological specifications of the wear-depth measurement system are summarized in Table 2, while the corresponding characteristics of the humidity, temperature, and production-flow measurement systems are presented in Tables 3-5, respectively.

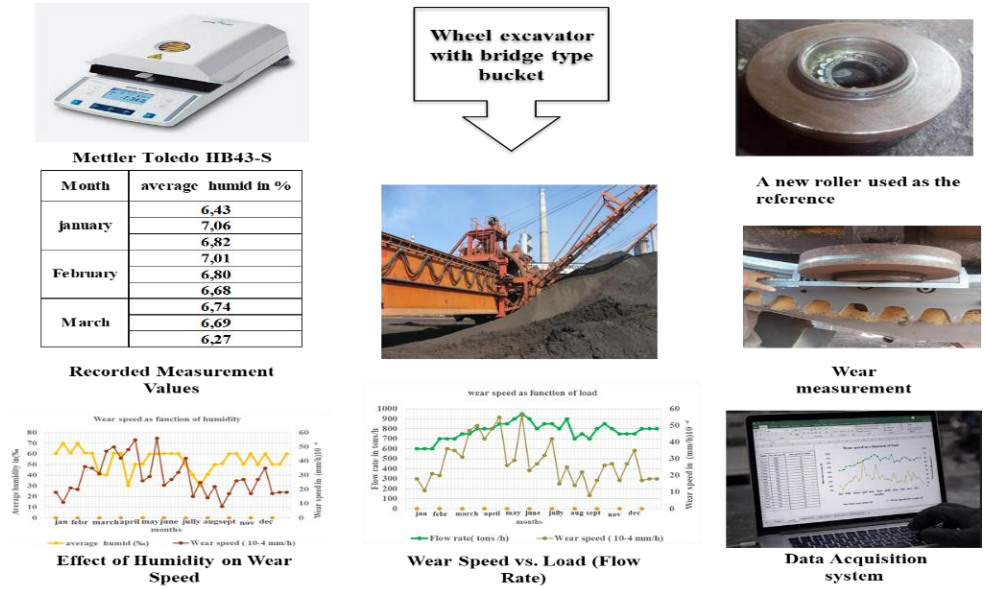

Figure 2. Wear measurement and data analysis protocol

Table 3. Metrological characteristics of the ore-moisture-content measurement system

Humidity	Specification
Instrument/System	Moisture analyzer
Range	0 – 100% RH
Resolution	0.01%
Accuracy/Uncertainty	±0.15% absolute
Calibration standard	ISO 3087:2020
Calibration interval	1 month

Table 4. Metrological characteristics of the temperature measurement system

Temperature	Specification
Instrument/System	Digital thermometer
Range	−10 to 60 °C
Resolution	0.1 °C
Accuracy/Uncertainty	±0.5 °C
Calibration standard	ISO 80601-2-56
Calibration interval	6 months

Table 5. Metrological characteristics of the production flow measurement system

Production Flow	Specification
Instrument/System	Process Indicator
Range	0 – 1500 t/h
Resolution	1 t/h
Accuracy/Uncertainty	±2% FS
Calibration standard	IEC 61518-1
Calibration interval	12 months

4.2 Measurement procedure and uncertainty budget

Wear measurements followed a standardized protocol involving three-point diameter measurement at 120° intervals for each roller. Each measurement was repeated three times by trained operators, with the mean value recorded as the representative measurement.

The uncertainty budget was established according to JCGM 100:2008 and ISO 13385-1:2011 requirements.

The measurement uncertainty was estimated following the Joint Committee for Guides in Metrology (JCGM) 100:2008 guidelines:

- Type A uncertainty (repeatability): ±0.05 mm (from 30 repeated measurements);
- Type B uncertainty (instrument): ±0.02 mm (from calibration certificate);
- Environmental factors: ±0.01 mm (temperature compensation applied);
- Combined standard uncertainty: $u_c = \sqrt{0.05^2 + 0.02^2 + 0.01^2} = 0.054$ mm, where u_c represents the overall standard uncertainty associated with the wear measurement after combining the contributions from repeatability, instrument accuracy, and environmental effects.
- Expanded uncertainty (k = 2, 95% confidence): U95 = ±0.11 mm.

4.3 Ore moisture content measurement system

Ore moisture content was measured using a precision moisture analyzer following ISO 3087:2020 for iron ore

moisture determination. Automatic cross-stream sampling was used to obtain representative material samples, and weekly verification was performed against certified reference materials. The measurement uncertainty associated with the ore moisture content was estimated as ±0.15% absolute moisture content. Throughout this manuscript, this variable is referred to as ore moisture content rather than environmental humidity.

4.4 Quality assurance measures

To ensure measurement reliability, multiple quality assurance measures were implemented:

1. Regular instrument verification using gauge blocks (Grade 0).
2. Inter-operator comparison studies showing ±0.03 mm consistency.
3. Environmental control during measurements (20±2 °C, 50±10% RH).
4. Complete documentation of measurement conditions for traceability.

5. STATISTICAL ANALYSIS FOR FAILURE DATA

5.1 Data origin and aggregation

The failure data used in this study were obtained from industrial maintenance and operational logs of the investigated bridge-type BWE under varying production-load conditions. Each recorded event corresponds to an actual maintenance intervention documented during operation. Because failure events at the individual-component level were relatively infrequent and unevenly distributed over time, the raw observations were grouped by operating-load range and aggregated over extended operating periods. The resulting grouped dataset was used for comparative statistical analysis. The statistical analysis was then conducted using analysis of variance (ANOVA) and Spearman's rank correlation to examine the association between operating load and failure occurrence. These analyses should therefore be interpreted as based on aggregated industrial field data rather than on a large set of independent raw failure events.

5.2 Correlation analysis between load and failure: An approach using the analysis of variance method

The statistical relationship between operating load and failure occurrence was evaluated using correlation analysis, and the corresponding coefficients and significance levels are reported in Table 6. The load-dependent mean failure rates for the bucket wheel, trolley, bridge, and total system are summarized in Table 7.

To enhance the robustness of the statistical analysis, failure data were aggregated over extended operating periods and reorganized into a larger dataset of size N = 30, reflecting the observed failure trends under different load levels. This approach enables the application of ANOVA while preserving the physical consistency of the original industrial observations, with a sufficient sample size (> 30 by the empirical rule for approximate normality).

Accordingly, the statistical results reported in this section support load-related trends within the grouped industrial dataset used in this study, but they should not be interpreted as establishing fully general effect sizes beyond the investigated case.

Table 6. Correlation analysis between operating load and failure occurrence

Variable Pair	Correlation Coefficient	P-Value	Interpretation
Load level – Failures (Subsystem 1: Bucket wheel)	0.78	< 0.01	Strong positive correlation
Load level – Failures (Subsystem 2: Trolley)	0.52	< 0.05	Moderate positive correlation
Load level – Failures (Subsystem 3: Bridge)	0.46	< 0.05	Moderate positive correlation
Load level – Total system failures	0.71	< 0.01	Strong positive correlation

Table 7. Load-dependent failure rates: Bucket wheel, trolley and bridge

Operating Load Level (t/h)	Mean Failures – Subsystem 1 (Bucket Wheel)	Mean Failures – Subsystem 2 (Trolley)	Mean Failures – Subsystem 3 (Bridge)	Mean Total System Failures
< 600	1.90	0.30	0.40	2.60
600 – 800	5.00	2.40	2.90	10.3
> 800	3.90	0.30	0.60	4.80

6. EXPERIMENTAL WEAR STUDY

The experimental program monitored four support rollers on the bucket-wheel carriage over an eleven-month observation period. Wear measurements were performed at regular intervals using the calibrated digital vernier caliper described in Section 4 and Table 2. In parallel, operating load (t/h) and average ore moisture content (%) were recorded for each observation period.

Figure 3. Wear measurement using a caliper

Figure 4. A new roller used as the reference

Figure 5. Worn rollers

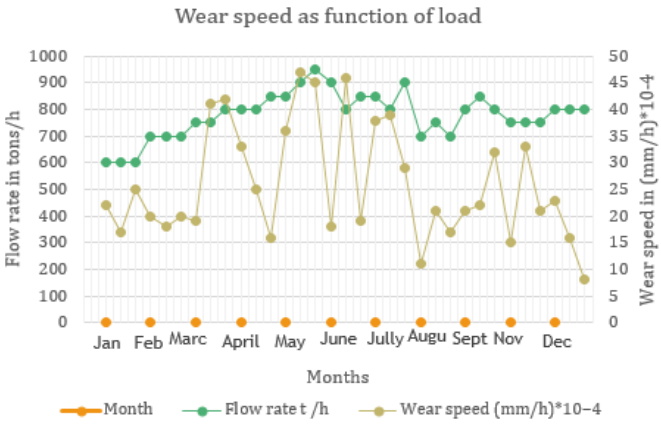

Figure 6. Variation of wear rate for roller 1 based on load

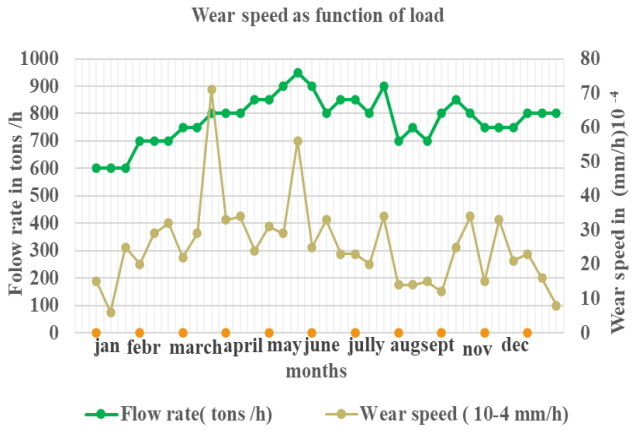

Figure 7. Variation of wear rate for roller 2 based on load

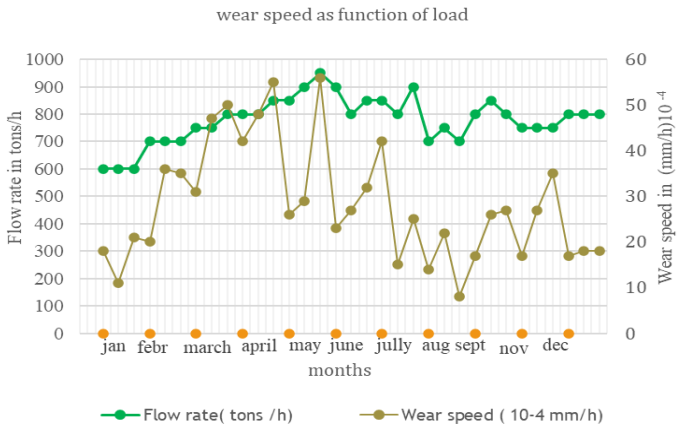

Figure 8. Variation of wear rate for roller 3 based on load

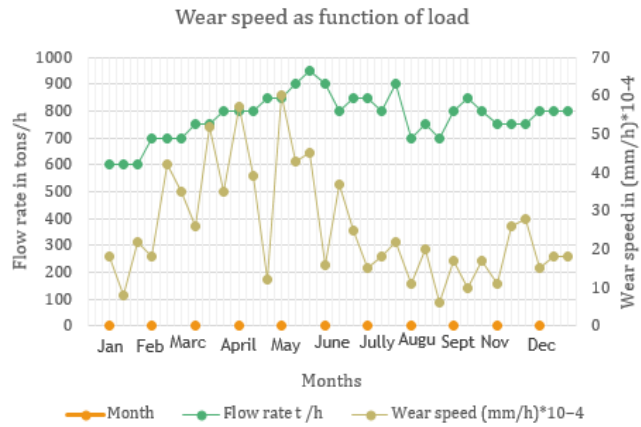

Figure 9. Variation of wear rate for roller 4 based on load

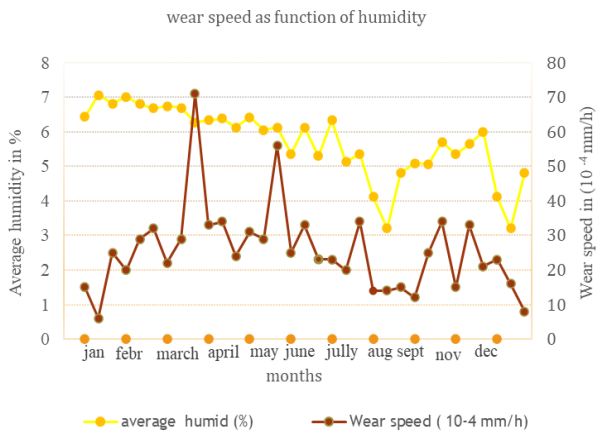

Figure 10. Variation of wear rate for roller 1 based on humidity

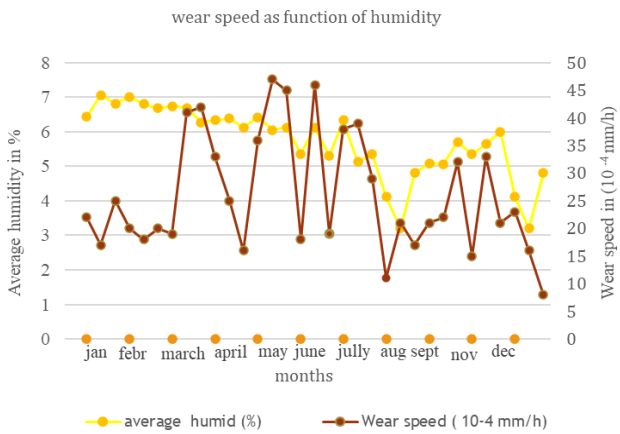

Figure 11. Variation of wear rate for roller 2 based on humidity

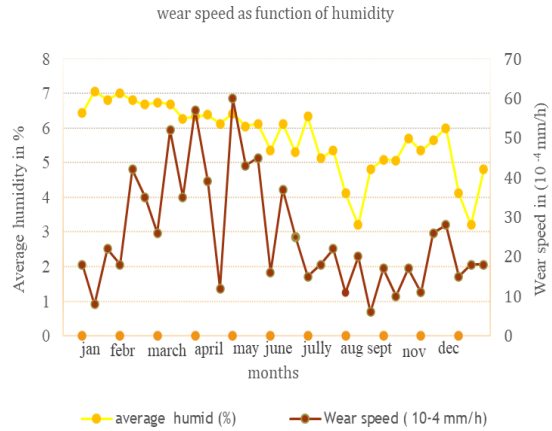

Figure 12. Variation of wear rate for roller 3 based on humidity

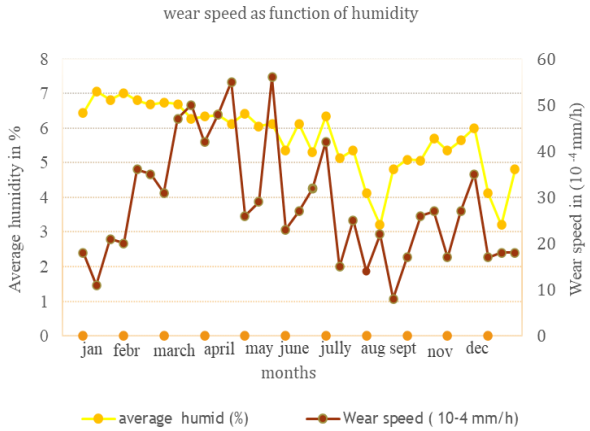

Figure 13. Variation of wear rate for roller 4 based on humidity

Figure 3 shows the experimental setup used for roller wear measurements. Figure 4 presents the new roller adopted as the unworn reference condition, and Figure 5 shows representative worn rollers after service exposure.

The increase of wear rate with operating load is consistent with previous tribological studies [15, 16].

The influence of operating load on wear evolution is presented in Figures 6-9, which depict the variation of wear rate for each roller as a function of production flow rate. These figures clearly show that wear rate increases with load, confirming the assumptions of the wear model.

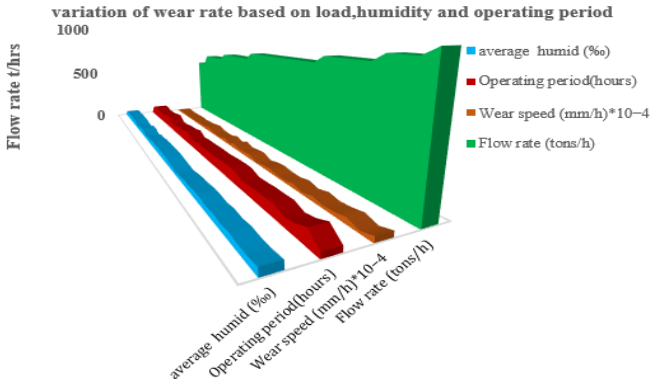

Figure 14. Variation of wear rate for roller 1 based on load, humidity and operating period

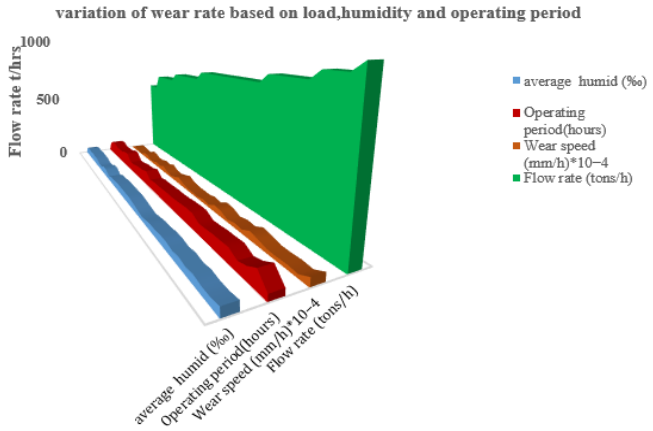

Figure 15. Variation of wear rate for roller 2 based on load, humidity and operating period

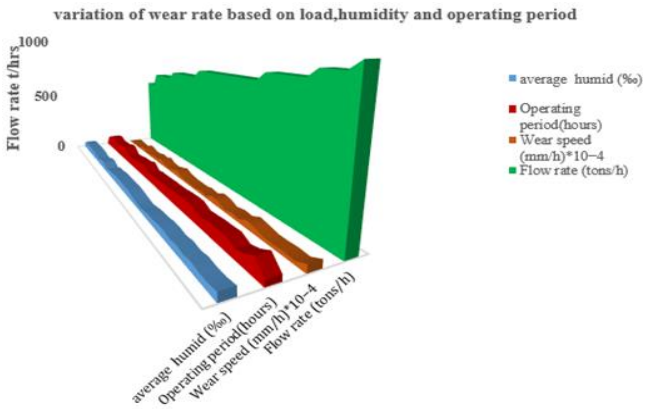

Figure 16. Variation of wear rate for roller 3 based on load, humidity and operating period

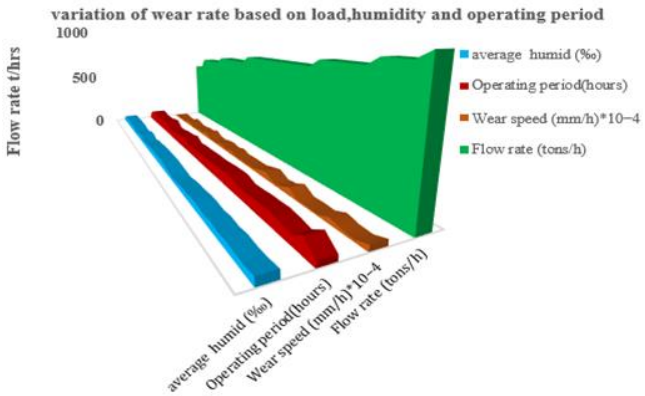

Figure 17. Variation of wear rate for roller 4 based on load, humidity and operating period

Similar moisture-related wear effects have been reported in previous studies [18, 19].

The effect of environmental humidity on wear is illustrated in Figures 10-13. The results indicate that higher humidity levels significantly accelerate wear due to corrosion-assisted abrasion mechanisms.

The combined effect of load and humidity on wear evolution is supported by previous tribological observations [10, 18, 19].

Finally, the combined influence of operating load, humidity, and operating time is presented in Figures 14-17. These three-

dimensional representations demonstrate that specific combinations of high load and elevated humidity lead to markedly increased wear rates, highlighting the interactive nature of these stressors.

7. SIMULATION-BASED PRODUCTION AND RELIABILITY ANALYSIS

A discrete-event simulation model was developed to analyze the dynamic behavior of the production line under degradation constraints. The logical structure of the simulation algorithm is summarized in Figure 18, which presents the flowchart of the proposed model, including machine states, accumulator levels, stochastic failure generation, and repair processes.

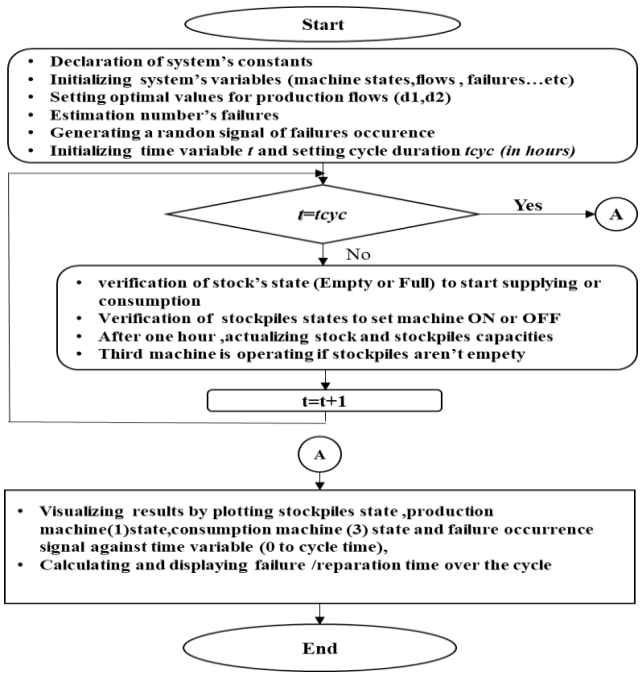

Figure 18. Flowchart of the new dynamic production line simulation algorithm

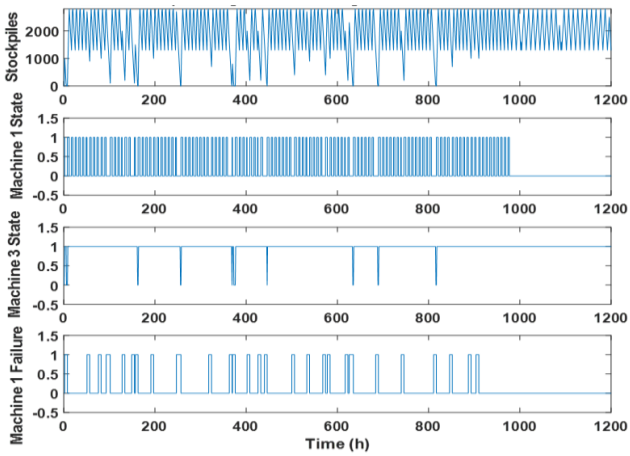

Figure 19. Machine operating condition with high flow rate and 20% failure rate

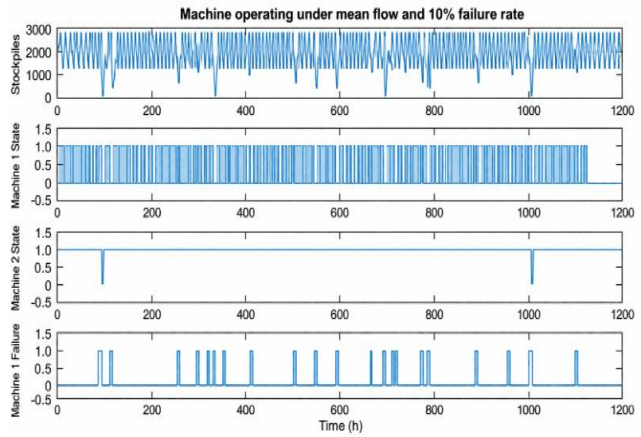

Figure 20. Machine operating condition with average flow rate and 10% failure rate

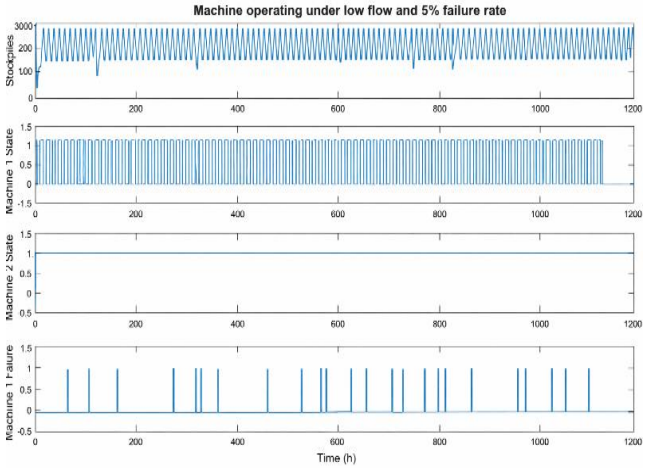

Figure 21. Machine operating condition with low flow rate and 5% failure rate

The simulation was used to evaluate system performance under three operating scenarios corresponding to low, medium, and high flow rates. The resulting machine operating conditions are illustrated in Figures 19-21, which show the evolution of machine states and failure occurrences over time for each scenario.

Table 8. Simulation table for the system with low flow rate

Test	NSLM for Machine M3	Machine M1 DT (hours)	Machine M1 MCT (hours)
Test 1	1	93	1121
Test 2	2	100	1125
Test 3	1	97	1125

Note: NSLM = Number of Stops due to Lack of Material; DT = Downtime; MCT = Mission completion time

Table 9. Simulation table for the system with average flow rate

Test	NSLM for Machine M3	Machine M1 DT (hours)	Machine M1 MCT (hours)
Test 1	14	209	1014
Test 2	13	193	996
Test 3	12	190	992

Note: NSLM = Number of Stops due to Lack of Material; DT = Downtime; MCT = Mission completion time

Table 10. Simulation table for the system with high flow rate

Test	NSLM for Machine M3	Machine M1 DT (hours)	Machine M1 MCT (hours)
Test 1	48	209	1134
Test 2	44	193	1136
Test 3	56	190	1138

Note: NSLM = Number of Stops due to Lack of Material; DT = Downtime; MCT = Mission completion time

Key performance indicators derived from the simulation include downtime (DT), mission completion time (MCT), and the number of system-level maintenance events. These indicators are summarized in Tables 8-10, enabling a quantitative comparison of reliability and productivity across different operating policies.

8. DISCUSSION

The results should be interpreted at three distinct levels. First, the wear-monitoring campaign provides direct observational evidence of progressive material loss in the four monitored support rollers under variable operating conditions. Second, the statistical analysis of historical failure records indicates that higher operating loads are associated with increased failure occurrence within the grouped industrial dataset considered in this study. Third, the interpretation of moisture-related effects is mechanism-based and should therefore be stated cautiously. In the revised manuscript, the variable previously referred to as humidity is defined as ore moisture content of the handled material rather than ambient relative humidity. The observed increase in wear under wetter operating conditions is therefore interpreted as being consistent with moisture-related aggravation of degradation, rather than as direct proof of a specific corrosion mechanism.

Taken together, the wear measurements, grouped failure records, and simulation results suggest that operating load and ore moisture content are important operating variables for degradation assessment in the investigated bridge-type BWE system. At the same time, these three sources of evidence do not have the same status. The wear data provide component-level measurements, the failure analysis is based on grouped industrial records, and the simulation translates these relationships into scenario-based system behavior. The discussion should therefore remain interpretive and case-specific rather than claiming universal parameter values or broadly transferable causal laws.

Differences observed among rollers or operating scenarios may reflect local contact conditions, operational heterogeneity, and the limited size of the monitored component set. For this reason, the discussion of anomalies should remain cautious and should not attribute any individual deviation to a specific mechanism unless that mechanism is independently documented by additional alignment, surface, or materials evidence.

The metrological framework implemented in this study provides a defined basis for interpreting the wear measurements. The expanded uncertainty of the wear measurement was estimated as ±0.11 mm at coverage factor k = 2, which supports the reliability of the measurement process and the comparability of repeated observations over time. However, measurement uncertainty should not by itself be interpreted as proof of statistical significance. Rather, it defines the confidence interval associated with the wear measurements and should be considered together with the observed magnitude and consistency of the wear trends.

Several limitations should be stated explicitly. First, the failure analysis is based on grouped industrial maintenance records, and the corresponding inferential results should therefore be interpreted cautiously rather than from a large set of independent raw events. Second, only four support rollers were monitored, so the wear data provide case-specific component-level evidence rather than a basis for broad generalization. Third, the study concerns one excavator system operating in one industrial context, which limits direct transferability to other machines, sites, materials, or service conditions. Fourth, the wear interpretation assumes approximately linear evolution over short observation intervals, which may not capture all transient effects. These limitations do not invalidate the present case study, but they define the scope within which its findings should be interpreted.

Nevertheless, limitations remain, including the relatively small failure dataset and the assumption of linear wear evolution over short operating intervals. Future work will focus on incorporating nonlinear, state-dependent degradation models and real-time condition monitoring data to enhance the predictive capability and industrial applicability of the approach.

A further limitation concerns the size of the wear-monitoring sample. Only four support rollers were monitored, and the corresponding measurements should therefore be interpreted as case-specific evidence for the investigated machine rather than as a basis for broad generalization to all BWEs or operating contexts. In the present study, the system-level implications are derived from the consistency observed between three sources of information: measured wear on the monitored rollers, grouped historical failure records, and discrete-event simulation results. Even so, transferability to other machines, sites, or material-handling conditions remains limited and should be examined in future studies using a broader component set and additional industrial cases.

9. CONCLUSION

This study highlights the importance of understanding the operating conditions associated with degradation in bridge-type BWEs used in iron-ore handling. The results indicate that higher operating loads and wetter service conditions are associated with faster degradation of critical components and with less favorable reliability outcomes.

The findings should therefore be interpreted as a case-study contribution that provides a measurement-grounded basis for reliability-informed maintenance assessment in the investigated excavator system, rather than as a broadly generalizable system model derived solely from the monitored roller sample.

Within the scope of the present case study, the simulation framework is intended to compare operating scenarios and their reliability implications. It should not be interpreted as a formal optimization algorithm for determining an optimal load policy. The main contribution of the study is therefore a measurement-grounded basis for reliability-informed maintenance assessment under variable operating conditions.

The analysis also highlights the influential roles of production rate and initial storage levels, which directly affect

overall system performance. A detailed investigation into the interactions among these parameters is essential for designing resilient systems capable of meeting production targets while mitigating risk. Furthermore, seasonal fluctuations in humidity call for environment-specific adaptive maintenance techniques. Maintaining equipment performance and structural integrity requires the implementation of particular preventive measures in response to climatic fluctuations.

To improve bucket excavators' longevity and operational efficiency, it is highly advised that these various factors be incorporated into their design, monitoring, and maintenance. A proactive and multifaceted approach to managing degradation in industrial excavation systems is supported by the convergence of environmental awareness, data-driven optimization, and algorithmic load control.

ACKNOWLEDGMENT

The authors acknowledge the support of the Central Metallurgy Laboratory.

REFERENCES

[1] Bošnjak, S.M., Arsić, M.A., Zrnić, N.Đ., Rakin, M.P., Pantelić, M.P. (2010). Bucket wheel excavator: Integrity assessment of the bucket wheel boom tie-rod welded joint. Engineering Failure Analysis, 18(1): 212-222. https://doi.org/10.1016/j.engfailanal.2010.09.001

[2] Wang, X.L., Xu, J.H., Zhang, L., Wang, N. (2023). Mission success probability optimizing of phased mission system balancing the phase backup and system risk: A novel GERT mechanism. Reliability Engineering & System Safety, 236: 109311. https://doi.org/10.1016/j.ress.2023.109311

[3] Bošnjak, S.M., Arsić, M.A., Gnjatović, N.B., Milenović, I.L., Arsić, D.M. (2017). Failure of the bucket wheel excavator buckets. Engineering Failure Analysis, 84: 247-261. https://doi.org/10.1016/j.engfailanal.2017.11.017

[4] Barabady, J., Kumar, U. (2008). Reliability analysis of mining equipment: A case study of a crushing plant at Jajarm Bauxite Mine in Iran. Reliability Engineering & System Safety, 93(4): 647-653. https://doi.org/10.1016/j.ress.2007.10.006

[5] Djurdjevic, D., Maneski, T., Milosevic-Mitic, V., Andjelic, N., Ignjatovic, D. (2018). Failure investigation and reparation of a crack on the boom of the bucket wheel excavator ERS 1250 Gacko. Engineering Failure Analysis, 92: 301-316. https://doi.org/10.1016/j.engfailanal.2018.05.015

[6] Lazarević, Ž., Aranđelović, I., Kirin, S. (2015). An analysis of random mechanical failures of bucket wheel excavator. Structural Integrity and Life, 15(3): 143-146.

[7] Branković, D., Milovanović, Z.N., Janičić-Milovanović, V. (2024). Reliability analysis of bucket-wheel excavator parts – Application of critical position selection algorithm. Journal of Graphic Era University, 13(1): 1-30. https://doi.org/10.13052/jgeu0975-1416.1311

[8] Arsić, M.A., Bošnjak, S.M., Odanović, Z.D., Dunjić, M.M., Simonović, A.M. (2011). Analysis of the spreader track wheels premature damages. Engineering Failure Analysis, 20: 118-136. https://doi.org/10.1016/j.engfailanal.2011.11.005

[9] Florea, V.A., Toderaș, M., Tihanov-Tănăsache, D. (2025). Influence of abrasive wear on reliability and maintainability of components in quarry technological equipment: A case study. Applied Sciences, 15(7): 3603. https://doi.org/10.3390/app15073603

[10] Archard, J.F. (1953). Contact and rubbing of flat surfaces. Journal of Applied Physics, 24(8): 981-988. https://doi.org/10.1063/1.1721448

[11] Halling, J., Burton, R.A. (1977). Principles of tribology. Journal of Lubrication Technology, 99(2): 305-306. https://doi.org/10.1115/1.3453090

[12] Blau, P.J. (2001). The significance and use of the wear coefficient. Tribology International, 34(9): 585-591. https://doi.org/10.1016/S0301-679X(01)00050-0

[13] Lin, C.W. (2024). Degradation and life prediction of mechanical equipment based on multivariate stochastic process. Frontiers in Mechanical Engineering, 10: 1418137. https://doi.org/10.3389/fmech.2024.1418137

[14] Meitz, L., Senge, J., Wagenhals, T., Schöler, T., Hähner, J., Edinger, J., Krupitzer, C. (2025). A literature review framework and open research challenges for predictive maintenance in Industry 4.0. Computers & Industrial Engineering, 206: 111193. https://doi.org/10.1016/j.cie.2025.111193

[15] Bhushan, B. (2013). Principles and Applications of Tribology (2nd ed.). John Wiley & Sons. https://doi.org/10.1002/9781118403020

[16] Villanueva, E., Albizuri, J., Caballero, P., Guraya, T., Vicario, I. (2025). Prediction of wear rate by a new direct method using the friction coefficient curve. Journal of Manufacturing and Materials Processing, 9(1): 6. https://doi.org/10.3390/jmmp9010006

[17] Rabinowicz, E. (1965). Friction and Wear of Materials. New York: Wiley.

[18] Liu, Z.L., Xiang, Z.Y., Xie, S.L., Liu, G.H., Tang, B., Wang, X.C., He, D.Q. (2025). The effect of environmental humidity on the friction-induced stick-slip vibration. Wear, 578: 206208. https://doi.org/10.1016/j.wear.2025.206208

[19] Chen, Z., He, X., Xiao, C., Kim, S.H. (2018). Effect of humidity on friction and wear—A critical review. Lubricants, 6(3): 74. https://doi.org/10.3390/lubricants6030074

NOMENCLATURE

NSLM	Number of Stops due to Lack of Material
MCT	Mission Completion Time
DT	Downtime
U95	Expanded measurement uncertainty (95% confidence level)
K	Coverage factor (typically k = 2 for 95% confidence)
ISO	International Organization for Standardization
JCGM	Joint Committee for Guides in Metrology
BWE	Bucket-Wheel Excavator

Symbols

L	Sliding distance, m
V	Worn volume, m^3
F_N	Load, N